Direct Retrieval of Stratospheric CO_2 Infrared Cooling Rate Profiles from AIRS Data

D.R. Feldman[1], K.N. Liou[2], Y.L. Yung[1], D.C. Tobin[3], and A. Berk[4]

[1] Department of Environmental Science and Engineering, California Institute of Technology, Pasadena, California, USA

[2] Department of Atmospheric and Oceanic Sciences, University of California, Los Angeles, California, USA

[3] Cooperative Institute for Meteorological Satellite Studies, University of Wisconsin, Madison, Wisconsin, USA

[4] Spectral Sciences, Inc., Burlington, Massachusetts, USA

Abstract

[1] We expand upon methods for retrieving thermal infrared cooling rate profiles, originally developed by Liou and Xue [1988] through application to the inversion of the stratospheric cooling rate produced by carbon dioxide (CO_2) and a formal description of the associated error budget. Specifically, we infer lower- and mid-stratospheric cooling rates from the CO_2 ν_2 band on the basis of selected spectral channels and available data from the Atmospheric Infrared Sounder (AIRS). In order to establish the validity of our results, we compare our retrievals to those calculated from a forward radiative transfer program using retrieved temperature data from spectra taken by the Scanning High-Resolution Interferometer Sounder (S-HIS) on two aircraft campaigns: the Mixed-Phase Arctic Cloud Experiment (MPACE) and the Aura Validation Experiment (AVE) both in Fall, 2004. Reasonable and consistent comparisons are illustrated, revealing that spectral radiance data taken by high-resolution infrared sounders can be used to determine the vertical distribution of radiative cooling due to CO_2.

1. Introduction

[2] Conventional clear-sky infrared cooling rates are calculated ubiquitously and the accuracy of these calculations has been shown to affect forecast and general circulation model (GCM) performance [*Iacono et al.*, 2000]. Numerical weather prediction models calculate radiative heating and cooling efficiently but are burdened by the computational requirement of estimating the atmospheric state from a suite of different instruments. In this light, novel approaches for the treatment of heating and cooling, especially from remote spectroscopic measurements, may be warranted. The largest infrared cooling takes place in the stratosphere and grid point temperature evolution in this region is strongly influenced by radiative interactions. The interaction between solar heating and infrared cooling has been analyzed theoretically by numerous studies and also in light of satellite instrument measurements [*Mlynczak et al.*, 1999]. However, since the infrared cooling rate profile is dependent upon individual layer atmospheric state vector values and their relationship to the broad structure of the atmospheric state, we seek to understand whether high-resolution infrared spectra can offer a better description of the infrared cooling rate profile beyond the atmospheric state standard products, especially in polar regions. If cooling rates can be successfully retrieved from the numerous spectra gathered by the current suite of Earth Observing System instruments, it may be possible to ingest these data into forecast models and GCMs. The retrieval of infrared cooling rates from top-of-atmosphere (TOA) radiance data is a novel concept and may improve upon the understanding of the vertical distribution of infrared radiative cooling if successfully implemented. The approach of this retrieval will differ from that of atmospheric state retrievals in that the quantity we seek to retrieve is determined by broad spectroscopic features of species with strong absorption bands that significantly affect Planck function emission. Therefore, the retrieval must analyze absorption band channels in the context of a channel's description of the

radiative cooling of that band at a certain level as opposed to a channel's description of an atmospheric state quantity at that level.

[3] We chose to demonstrate the feasibility of a cooling rate profile retrieval with the CO_2 ν_2 band as measured by the AIRS instrument [*Aumann et al.*, 2003] for several reasons. First, the CO_2 ν_2 band is a major contributor to clear-sky cooling in the stratosphere and mesosphere [*Kiehl and Solomon*, 1986]. Second, CO_2 is quite well-mixed and the cooling rate profile does not vary substantially over an observation granule. Third, AIRS is a proven instrument with extensive spatial coverage, unrivaled signal-to-noise ratio, and well-quantified stability [*Aumann et al.*, 2005]. Finally, clouds, which greatly affect cooling rate profile values, are a minimal presence in the stratosphere so that the retrieval of CO_2 cooling rates can be greatly simplified.

[4] Calculations of the radiative cooling of CO_2 in the stratosphere are straightforward with known atmospheric state quantities, but uncertainties in some of these quantities, most notably the temperature structure, propagate into cooling rate errors in ways that have not been explored. A formal understanding of the cooling rate error budget through observation is therefore warranted in order to determine to what extent our method can improve cooling rate profile determination.

2. Theoretical Basis

[5] The derivation of the cooling rate profile from observed radiance data was first developed theoretically by Liou and Xue [1988] and improved by Liou [2002] in order to measure the strong tropospheric cooling produced by the rotational band of water vapor in the far infrared.

[6] The spectral cooling rate profile is defined by

$$\dot{\theta}(\nu,z)=\frac{1}{\rho(z)C_p}\frac{dF^{net}(\nu,z)}{dz}, \tag{1}$$

where $\dot{\theta}(\nu, z)$ is the cooling rate, $\rho(z)$ is the atmospheric density profile, C_p is the heat capacity of air at constant pressure, and $F^{net}(\nu, z)$ is the net flux at height z for wavenumber ν. The relationship between the Top-of-Atmosphere (TOA) flux, the flux-divergence profile, and TOA radiance is given by the following:

$$F^{+}(\nu, z=\infty) = F^{+}(\nu, z=0) + \int_0^{\infty} \frac{dF^{net}(\nu, z')}{dz'} dz', \tag{2a}$$

$$F^{+}(\nu, z=\infty) = 2\pi \int_0^{1} I(\nu, \mu, z=\infty)\mu \, d\mu, \tag{2b}$$

where $F^{+}(\nu, z)$ is the upwelling flux, z = 0 denotes the surface, $I(\nu, \mu, z)$ is the spectral radiance, and μ is the cosine of viewing zenith angle. Conventionally, the cooling rate profile is calculated for the entire infrared (0-3000 cm^{-1}) which can be derived by integrating Eq. (1) over a spectral region with respect to wavenumber. The contribution to the total infrared cooling rate of a spectral region at a particular level is given by the cumulative spectral cooling rate function which is defined as

$$\dot{\Theta}(\nu, z) = \frac{\int_0^{\nu} \dot{\theta}(\nu, z) d\nu}{\int_0^{\nu_{\max}} \dot{\theta}(\nu, z) d\nu}. \tag{3}$$

As shown in Fig.1, a change in color at a certain level on the horizontal axis implies appreciable spectral contribution to the total cooling rate value at that level.

[7] A formal relationship between the infrared cooling rate profile and measured radiance values for an spectral band was established in Liou and Xue [1988] and is given by the following:

$$\int_0^{\infty} K(\nu, \mu, z)\, \dot{\theta}(z)\, dz = \alpha(\nu, \mu) \bar{I}(\bar{\mu}) + \beta(\nu, \mu) I(\nu, \mu) = y(\nu, \mu), \tag{4}$$

where $K(\nu, \mu, z) = C_p \, \rho(z) T(\nu, \mu, z)$ forms the weighting function matrix, $T(\nu, \mu, z)$ is the transmittance function, $I(\nu, \mu)$ is the TOA radiance, the coefficients $\alpha(\nu, \mu)$ and $\beta(\nu, \mu)$ can be determined numerically, and $\bar{I}(\bar{\mu})$ is the mean spectral radiance as measured at a zenith angle, $\bar{\mu}$, computed from the mean value theorem (see Liou and Xue [1988] for derivation). In this paper, the values of $\alpha(\nu,\mu)$ and $\beta(\nu,\mu)$ are computed numerically from two executions of our radiative transfer model at slightly different atmospheric states. Each value of the measurement metric $y(\nu,\mu)$ corresponds to the convolution of the cooling rate profile with the channel weighting function. The values of $\alpha(\nu,\mu)$ and $\beta(\nu,\mu)$ relate radiances to spectral-integrated and spectrally-independent TOA fluxes. Equation (4) demonstrates that the cooling rate profile cannot be measured in a forward sense with a remote spectrometer, but it is physically possible to derive information about the profile from TOA radiance measurements using inverse theory based on the Fredholm equation of the first kind denoted in Eq. (4).

[8] Assuming that the functional relationship between the measurements and the retrieval is well-behaved in the solution region, Eq. (4) can be analyzed using a linear Bayesian estimation technique to retrieve cooling rate profile. With Gaussian statistics for the measurement and *a priori* error, the retrieved state can be expressed as a balance between the expected amount of information about the retrieval quantity as given by the measurement metric $y(\nu,\mu)$ with the information that constrains the retrieval to a certain solution space. The *a priori* covariance matrix of the cooling rate profile which is utilized to constrain the retrieval is calculated empirically given expected state vector changes values in the cross-track path. For the cooling rate profile *a priori* constraint, the long range covariances between cooling rate profile components are smoothed according to a scale-height correlation that is derived from the near off-diagonal components of the empirical covariance matrix. The error covariance matrix which describes expected errors in the measurement metric is assumed to be a diagonal matrix with diagonal elements derived from the expected deviation in measurements derived from Eq. (4). For this type of retrieval error analysis,

it can be shown (Rodgers [2000]) that the *a posteriori* covariance for the cooling rate profile can then be determined by analyzing the combination of the measurement error projected onto the data space and the prior error.

[9] In terms of computing the net flux divergence at several atmospheric levels, radiance measurements at different viewing angles provide improved information over a single sounding, but the degree and manner in which angular information can be utilized needs to be explored further. According to Liou and Xue [1988], the cooling rate profile can be derived from measurements at 2 viewing angles, but it is important to generalize their findings for more complicated scenarios with cross-track spatial variability where the viewing geometry does not easily lend itself to meaningful spatial resolution. Various measurements may be utilized according to the viewing geometry of instrument being considered, but it must be remembered that for scanning instruments, radiance values taken at different viewing angles describe unique atmospheric states. Nevertheless, knowledge of the spatial covariance in cooling rate profiles over short scales will allow us to estimate cooling rate profiles more robustly. The utilization of angular radiance values represents a balance between the need for more cooling rate profile details than can be derived from the radiance at a single viewing angle and the lack of correlation between different atmospheric states from different viewing angles.

[10] The measurement metric through which the cooling rate profile is retrieved, $\mathbf{y}$, must be modified to include an optimal amount of the cross-track angular scan as determined by the error budget considerations described above. As such, $\mathbf{y}$, vectorized according to wavenumber, is defined as

$$\mathbf{y} = [\mathbf{y}(\mu_o) \quad \cdots \quad \mathbf{y}(\mu_n)] \,, \tag{5a}$$

$$\mathbf{y}(\mu_i) = \int_0^\infty \left(\rho(z) C_p \mathbf{T}(\mu_i, z)\right) \dot{\theta}(z)\, dz \,, \tag{5b}$$

where $\mathbf{T}(\mu_i, z)$ is the transmittance as a function of viewing angle and height vectorized by wavenumber, and the i subscript refers to a discrete viewing angle in a cross-track scan. The metric $\mathbf{y}$ must be defined in such a way as to maximize the information content that can be derived about the integrand. The multiplication factors relating Eq. (4) to measured radiances are given by the following:

$$\mathbf{y}(\mu_i) = \boldsymbol{\gamma}(\mu_i)\mathbf{I}(\mu_i) \ . \tag{6}$$

The angular weighting terms $\boldsymbol{\gamma}(\mu_i)$ are also vectorized according to wavenumber and are calculated in a similar manner as $\alpha(\nu, \mu)$ and $\beta(\nu, \mu)$ as listed above. The formal measurement error covariance matrix then becomes the sum of two terms: The first is derived from the radiometric uncertainty multiplied by the angular weighting terms and the second term arises from an understanding of the *a priori* covariance of the cooling rate profile at the viewing angle μ_i with respect to the cooling rate profile of the footprint of interest at viewing angle μ_o. These two quantities determine the extent of the cross-track scan that can be utilized to retrieve cooling rate profiles.

3. Methods

[11] For radiance and transmittance calculations, we use Modtran™ 5, Version 2, Release 1[*Berk et al.*, 1989], which is a pre-release product offering spectral resolution as high as 0.1 cm^{-1}. The results of this program are routinely verified using the Line-by-Line Radiative Transfer Model version 9.3 (LBLRTM) and RADSUM 2.4 calculations [*Clough and Iacono*, 1995; *Clough et al.*, 2005] and generally agree to within 0.05 K/day between 800 and 5 mbar.

[12] Forward model radiances are convolved with the pre-launch AIRS Spectral Response Function (SRF) information [*Strow et al.*, 2003] to simulate AIRS channel measurements. For

Noise-effective Radiance (NeR), we use values derived from in-orbit calibration algorithms as included in the Level 1B data set [*Pagano et al.*, 2003]. We have calculated the cooling rate weighting functions for the AIRS instrument and found significant lower- and middle-stratospheric coverage from the 649 to 800 cm^{-1} region as shown in Fig.2. In this figure, the normalized cooling rate weighting functions for 453 AIRS channels with about 1 cm^{-1} FWHM per channel cover a large portion of the CO_2 ν_2 band spectral interval and their cooling rate weighting functions cover from the surface to 1 mbar. The cooling rate profile multiplied by the channel weighting function yields the amount cooling rate signal in each channel.

4. Cross-Comparison

[13] Direct validation of cooling rate profile retrievals requires data from *in situ* vertically ascending or descending hemispheric radiometers that span the spectral region of interest and that have the same overpass time as the remote sounder. In the absence of such a dedicated mission, only a cross-comparison between data sets is possible. We do this by analyzing other sets of coincidental spectra and deriving atmospheric state information, and then inputting that data into the forward model to calculate the cooling rate profile.

[14] We utilize data from Scanning High-Resolution Interferometer Sounder (S-HIS) taken during AVE over the Gulf of Mexico and the southeastern United States during October, 2004 [*AVE*, 2005; *Revercomb*, 1998]. These data include zenith and nadir soundings at altitudes from 10-20 km aboard a NASA WB-57 aircraft coincidental with Aqua and Aura overpasses. The instrument model for S-HIS and AIRS are distinct: the SRF of the S-HIS instrument is given by a sinc function with an FWHM of 0.96 cm^{-1}. S-HIS measurement noise is calculated using spectra of the instrument's calibration black-body.

[15] We have calculated the cooling rate profile in the 649 to 800 cm^{-1} region by using the forward model with a retrieved temperature and CO_2 profile from the S-HIS zenith and nadir spectra. The retrieved atmospheric state is calculated using a linear Bayesian update similar to Eq. (4). The *a priori* cooling rate profile is calculated from AIRS L2 standard retrieval product data with an assumed uniform CO_2 profile of 379 ppmv. Uncertainties in the *a priori* and measured profiles were derived empirically by varying the atmospheric state vector according to the L2 estimated errors in state vector components. The uncertainty in the retrieved cooling rate profile is given by a standard *a posteriori* covariance matrix for a linear retrieval (see Rodgers [2000] for details). The error covariance matrix is calculated according to radiometric error estimation and cross-track temperature changes in the L2 granule data. A comparison of the measured, *a priori*, and retrieved profiles is shown in Fig. 3a and suggests that our methods may be utilized for a more extensive analysis of the CO_2 cooling rate profile. Discrepancies between measurements and *a priori* cooling rate values arise from water vapor contribution at the far wing of the ν_2 band and surface temperature and emissivity uncertainties.

[16] Because there is greater uncertainty in stratospheric cooling processes in polar regions, we also performed a cross-comparison test using data from the MPACE mission near Fairbanks, Alaska aboard a Proteus aircraft flying at 11 km [*Harrington and Verlinde*, 2004]. As shown in Fig. 3b, the agreement between retrieved and measured cooling rate profiles is sufficient in the lower stratosphere, but is insufficient in the free troposphere largely due to the difficulties associated with temperature retrievals at high latitudes.

5. Discussion

[17] The concept of a direct retrieval of radiative cooling profiles in the infrared is relatively uncharted territory and this vein of research presents several exciting opportunities for future work.

We have expanded upon the original work relating radiance measurements to atmospheric cooling rate profiles so that real data are used, and two cross-comparison experiments lend confidence to the methods that we utilize. Stratospheric cooling rates caused by CO_2 are assumed to be known currently to within a few tenths of a K/day, but the uncertainty has yet to be formally quantified in light of temperature uncertainties. Our retrievals are generally precise to within 0.1 K/day in the lower and middle-stratosphere. Unfortunately, the AIRS instrument does not cover the entire CO_2 ν_2 band, and the scaling between partial band and total band cooling needs to be explored further.

[18] The stratospheric temperature decrease in winter- and spring-time polar regions is of great scientific interest because of the interaction between radiative and dynamic effects in this region. The total stratospheric cooling rate profile meridional variation near the polar region has been explored briefly [*Hicke et al.*, 1999] using similar methods to the cross-comparison of *in situ* data described above, though our utilization of zenith spectra is novel. The results of these works indicate that changes in the cooling rate profile of the lower stratosphere in polar regions will be detectable if the retrieval can be precise to around 0.1 K/day.

[19] A thorough analysis of stratospheric radiative cooling rates to measure the trends in radiative cooling due to changing stratospheric climate and CO_2 concentrations will require a robust input data set that resolves temperature profiles from the tropopause to the middle stratosphere. It will also require the development of computationally-efficient methods for calculating the angular weighting terms $\gamma(\mu_i)$ and a thorough understanding of the effects of errors in these values on retrieved cooling rate profiles. Ultimately, an operational algorithm for the ingestion of radiance information into cooling rate calculations for numerical weather prediction would be a monumental task and a computationally-efficient and accurate scheme for doing so has been proposed here.

Acknowledgements

[20] We would like to acknowledge the following individuals for their assistance with this research: David Rider, Jack Margolis, and George Aumann of JPL, Tony Clough from AER, Gail Anderson of the NOAA and Xun Jiang, Vijay Natraj, Run-Lie Shia and Xin Guo of the Caltech. D.R. Feldman’s research was supported in part by NASA grant NNG04GD76G and the AIRS Project at JPL. A.Berk’s collaboration was supported by AFRL/BAA FA8718-04-C-0073.

References

Aumann, H.H., M.T. Chahine, C. Gautier, M.D. Goldberg, E. Kalnay, L.M. McMillin, H. Revercomb, P.W. Rosenkranz, W.L. Smith, D.H. Staelin, L.L. Strow, and J. Susskind, AIRS/AMSU/HSB on the aqua mission: Design, science objectives, data products, and processing systems, *Ieee Transactions on Geoscience and Remote Sensing*, *41* (2), 253-264, 2003.

Aumann, H.H., D. Gregorich, and S. Gaiser, AIRS hyper-spectral measurements for climate research: Carbon dioxide and nitrous oxide effects, *Geophysical Research Letters*, *32* (5), 2005.

AVE, AURA Validation Data Center (http://avdc.gsfc.nasa.gov), NASA, Greenbelt, MD, 2005.

Berk, A., L.S. Bernstein, and D.C. Robertson, MODTRAN: A moderate resolution model for LOWTRAN 7, pp. 38, AFGL, 1989.

Clough, S.A., and M.J. Iacono, Line-by-Line Calculation of Atmospheric Fluxes and Cooling Rates .2. Application to Carbon-Dioxide, Ozone, Methane, Nitrous-Oxide and the Halocarbons, *Journal of Geophysical Research-Atmospheres*, *100* (D8), 16519-16535, 1995.

Clough, S.A., M.W. Shephard, E. Mlawer, J.S. Delamere, M. Iacono, K. Cady-Pereira, S. Boukabara, and P.D. Brown, Atmospheric radiative transfer modeling: a summary of the AER codes, *Journal of Quantitative Spectroscopy & Radiative Transfer*, *91* (2), 233-244, 2005.

Harrington, J., and J. Verlinde, Mixed-Phase Arctic Cloud Experiment Science Document, (http://nsa.met.psu.edu/verlinde/mpace/sciencedoc.pdf), pp. 28, The Pennsylvania State University, State College, Pa., 2004.

Hicke, J., A. Tuck, and H. Vomel, Lower stratospheric radiative heating rates and sensitivities calculated from Antarctic balloon observations, *Journal of Geophysical Research-Atmospheres*, *104* (D8), 9293-9308, 1999.

Iacono, M.J., E.J. Mlawer, S.A. Clough, and J.J. Morcrette, Impact of an improved longwave radiation model, RRTM, on the energy budget and thermodynamic properties of the NCAR community climate model, CCM3, *Journal of Geophysical Research-Atmospheres*, *105* (D11), 14873-14890, 2000.

Kiehl, J.T., and S. Solomon, On the Radiative Balance of the Stratosphere, *Journal of the Atmospheric Sciences*, *43* (14), 1525-1534, 1986.

Liou, K.N., *An introduction to atmospheric radiation*, 583 pp., Academic Press, Boston, 2002.

Liou, K.N., and Y.K. Xue, Exploration of the Remote Sounding of Infrared Cooling Rates Due to Water-Vapor, *Meteorology and Atmospheric Physics*, *38* (3), 131-139, 1988.

Mlynczak, M.G., C.J. Mertens, R.R. Garcia, and R.W. Portmann, A detailed evaluation of the stratospheric heat budget - 2. Global radiation balance and diabetic circulations, *Journal of Geophysical Research-Atmospheres*, *104* (D6), 6039-6066, 1999.

Pagano, T.S., H.H. Aumann, D.E. Hagan, and K. Overoye, Prelaunch and in-flight radiometric calibration of the Atmospheric Infrared Sounder (AIRS), *Ieee Transactions on Geoscience and Remote Sensing*, *41* (2), 265-273, 2003.

Revercomb, H., Recent Results from Two New Aircraft-Based Fourier-Transform Interferometers, in *ASSFTS Conference*, Toulouse, France, 1998.

Rodgers, C.D., *Inverse Methods for Atmospheric Sounding: Theory and Practice*, 256 pp., World Scientific, London, 2000.

Strow, L.L., S.E. Hannon, M. Weiler, K. Overoye, S.L. Gaiser, and H.H. Aumann, Prelaunch spectral calibration of the Atmospheric Infrared Sounder (AIRS), *Ieee Transactions on Geoscience and Remote Sensing*, *41* (2), 274-286, 2003.

Figure Captions

Figure (1): Spectral cumulative contribution function for mid-latitude summer conditions. Values in excess of unity are allowed for levels where spectral heating occurs at higher wavenumbers.

Figure (2): Normalized cooling rate weighting functions for mid-latitude summer (MLS) conditions for AIRS instrument from 649 to 800 cm^{-1}.

Figure (3a) and (3b): Deviation from *a priori* cooling rate profile from 649-800 cm^{-1} for AIRS retrieved and S-HIS calculated cooling rate profiles. Black solid line: *a priori* cooling rate profile (lower axis); black dashed line: zero line for difference from *a priori*; blue line: cooling rate profile deviation from *a priori* calculated from S-HIS zenith and nadir measurements; red line: cooling rate profile deviation from *a priori* retrieved with AIRS L1B spectra from coincidental footprint and at 45° in the cross-track scan. (a): AVE Flight: 10/31/2004, 24.8 N, 271.8 E. (b): MPACE flight: 10/10/2004, 62.7 N, 214.4 E.

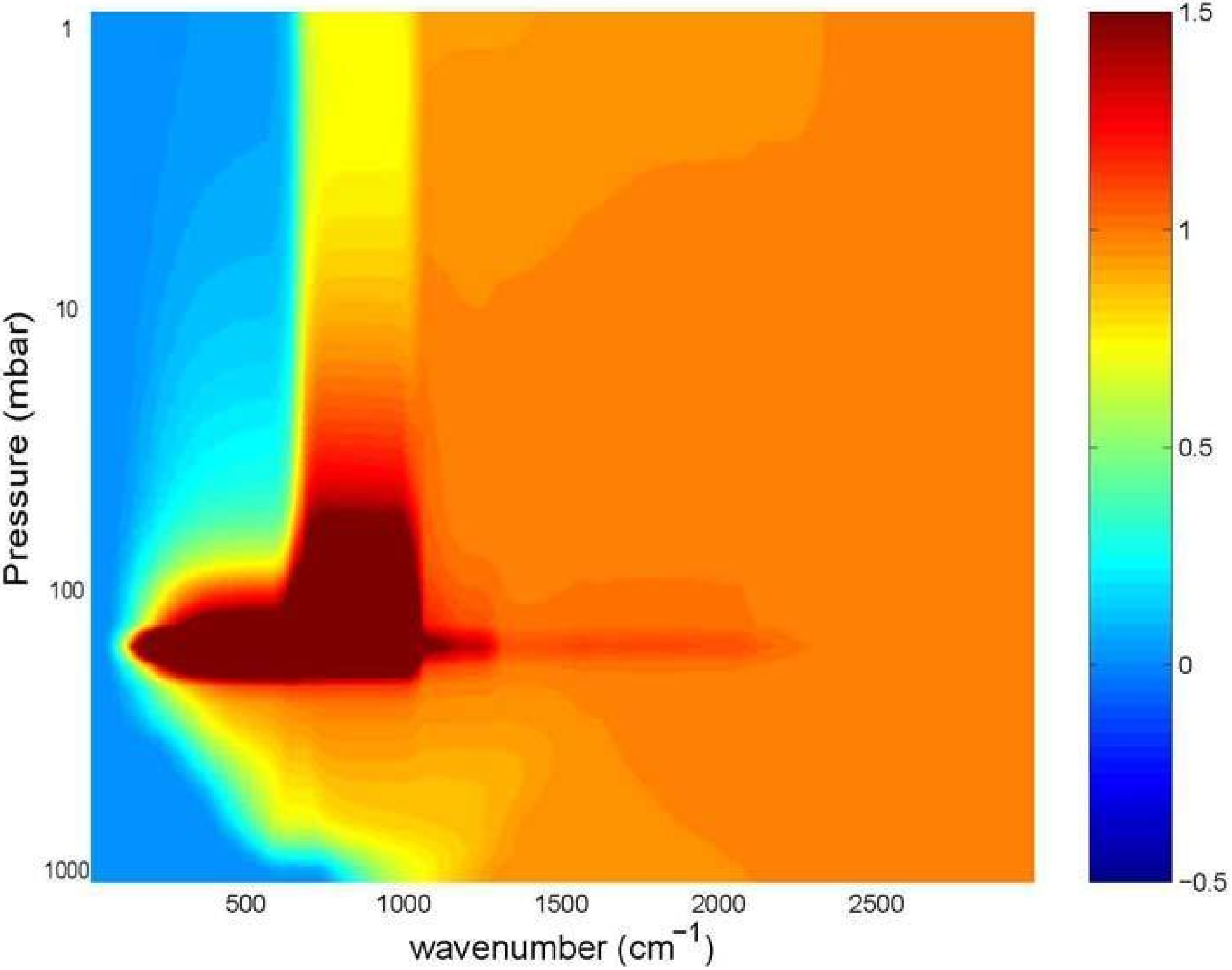
1
10
100
1000
Pressure (mbar)
500
1000
1500
2000
2500
wavenumber (cm^{-1})
1.5
1
0.5
0
−0.5

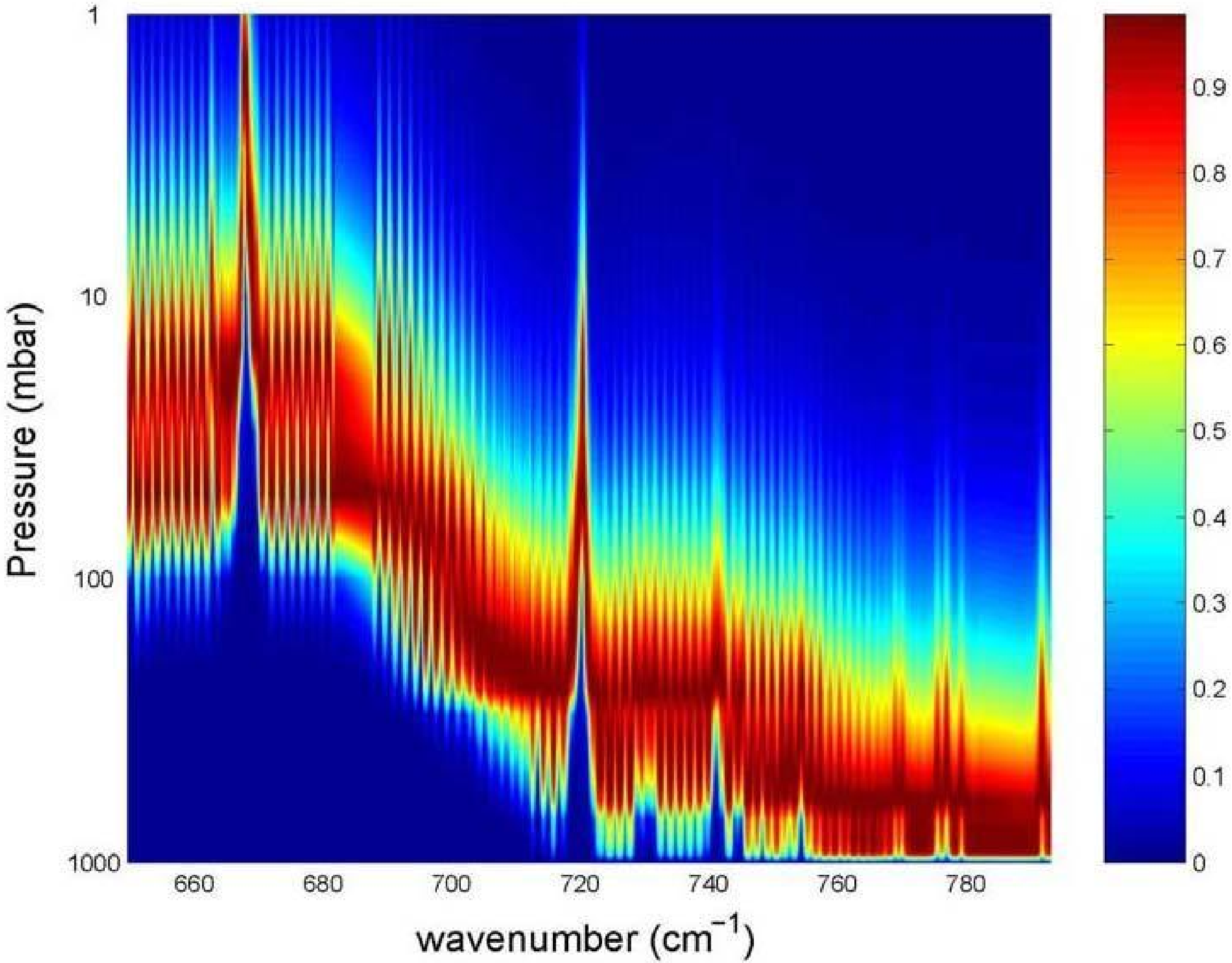
1
10
100
1000
Pressure (mbar)
660
680
700
720
740
760
780
wavenumber (cm^{-1})
0.9
0.8
0.7
0.6
0.5
0.4
0.3
0.2
0.1
0

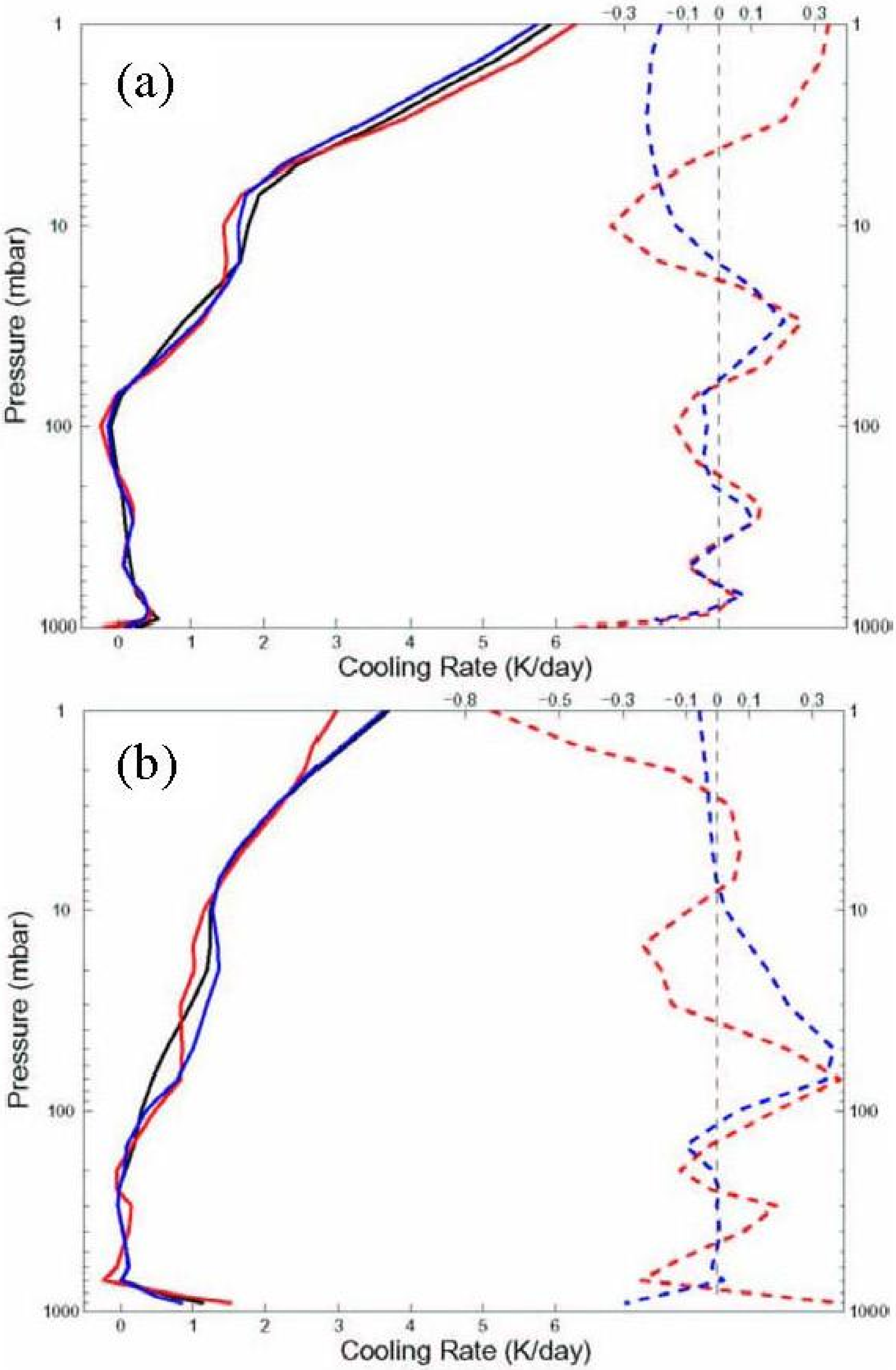
(a)
Pressure (mbar)
1
10
100
1000
Cooling Rate (K/day)
0
1
2
3
4
5
6
-0.3
-0.1
0
0.1
0.3
(b)
Pressure (mbar)
1
10
100
1000
Cooling Rate (K/day)
0
1
2
3
4
5
6
-0.8
-0.5
-0.3
-0.1
0
0.1
0.3